ACS APPLIED MATERIALS & INTERFACES

www.acsami.org

Research Article

Novel Porous Organic Polymer for the Concurrent and Selective Removal of Hydrogen Sulfide and Carbon Dioxide from Natural Gas Streams

Mahmoud M. Abdelnaby, Kyle E. Cordova, Ismail Abdulazeez, Ahmed M. Alloush, Bassem A. Al-Maythalony, Youcef Mankour, Khalid Alhooshani, Tawfik A. Saleh, and Othman Charles S. Al Hamouz*

Cite This: https://dx.doi.org/10.1021/acsami.0c14259

Read Online

ACCESS | Metrics & More | Article Recommendations | Supporting Information

ABSTRACT: Natural gas sweetening currently requires multistep, complex separation processes to remove the acid gas contaminants, carbon dioxide and hydrogen sulfide. In addition to being widely recognized as energy inefficient and cost-intensive, the effectiveness of this conventional process also suffers considerably because of limitations of the sorbent materials it employs. Herein, we report a new porous organic polymer, termed KFUPM-5, that is demonstrated to be effective in the concurrent separation of both hydrogen sulfide and carbon dioxide from a mixed gas stream at ambient conditions. To understand the ability of KFUPM-5 to selectively capture these gas molecules, we performed both pure-component thermodynamic and mixed gas kinetic adsorption studies and correlated these results with theoretical molecular simulations. Our results show that the underlying polar backbone of KFUPM-5 provides favorable adsorption sites for the selective capture of these gas molecules. The outcome of this work lends credence to the prospect that, for the first time, porous organic polymers can serve as sorbents for industrial natural gas sweetening processes.

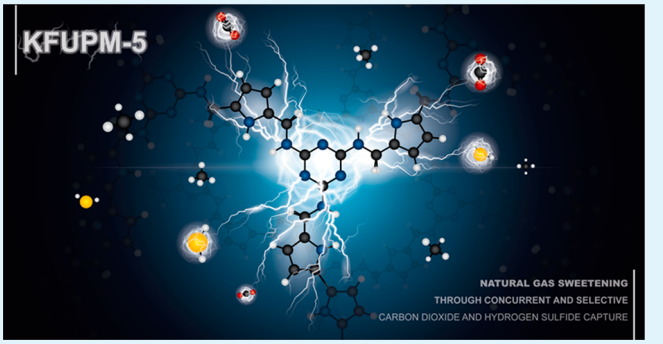

KEYWORDS: *porous organic polymers, porous materials, natural gas sweetening, hydrogen sulfide removal, carbon dioxide capture, dynamic separation*

INTRODUCTION

The main component of natural gas, methane, has attracted much interest as an alternative fuel source to the traditional petroleum-derived products, diesel and gasoline. Methane is naturally abundant, representing approximately two-thirds of fossil fuels on earth; it has a high research octane number, and because of its high H-to-C ratio, its emissions profile is much cleaner than other fossil fuels.[1,2] However, for methane to be practically useful for energy generation, the natural gas it originates from must be purified to remove unacceptable amounts of acid gas contaminants that are present (H_2S and CO_2).[1] After condensing out heavier hydrocarbons, the standard process for "sweetening" natural gas (i.e., removing acid gases) is to subject the gas stream to scrubbing units typically composed of liquid amine-based sorbents.[3] Although such scrubbing units and the liquid sorbents that comprise them have proven effective to a certain degree, they do present complex challenges, lead to prohibitive regeneration energy costs due to high specific heat capacities, and have shorter lifetimes as a result of sorbent poisoning.[3−8] Furthermore, liquid amine-based sorbents often suffer from H_2S/CO_2 selectivity challenges that are difficult to control due to differences in concentrations of these gas contaminants depending on where the natural gas originates.[4,5] Improvement of these sorbents is fundamentally important for realizing a higher performing sweetening process, yet, such improvement has been stymied because of an inherent lack of control in further altering the structures of these liquid amine-based sorbents beyond what has already been accomplished. Therefore, the main challenge of improving the natural gas sweetening process is a material one.

When considering future material design, it is crucial to understand the properties that must be fundamentally achieved. In an ideal scenario, these are as follows:[3,9] (i) Permanent porosity leading to high uptake capacity. High

Received: August 7, 2020
Accepted: September 28, 2020
Published: September 28, 2020

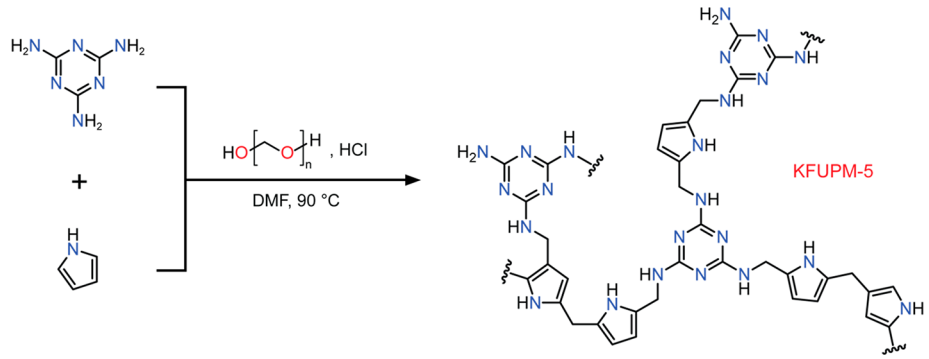

Figure 1. Synthesis of the novel porous organic polymer, KFUPM-5, reported herein. Through an acid-catalyzed polycondensation reaction, melamine and pyrrole were cross-linked via *p*-formaldehyde.

uptake capacity must be realized at the relevant partial pressures of the targeted acid gases in natural gas streams. (ii) High selectivity toward both H_2S and CO_2 as the employed sorbent should be capable of removing both of these concurrently.[4,5] This is difficult given that both gases are acidic in nature and, therefore, will likely compete for the same adsorption sites.[3] (iii) Long-term chemical stability. The presence of H_2S, both alone and together with CO_2, in natural gas streams creates hard-to-overcome reactivity challenges that the sorbent must withstand. (iv) Fast adsorption kinetics to realize industrially viable implementation. This means that a sorbent must not only perform well in pure-component thermodynamic adsorption settings but also in dynamic adsorption environments, where the presence of other gas molecules may impact adsorption properties.[10] (v) Mild, energy-efficient regeneration conditions[11] and (vi) low-cost production of the sorbent material. Realizing a sorbent material that satisfies these criteria would substantially simplify the number of separation steps, considerably lower costs, and improve the energy efficiency of the sweetening process, among others.[3]

Historically, metal oxides were explored in this regard, and though several specific types (e.g. zinc oxide,[12] ferric oxyhydroxide,[13] iron−zinc and iron−cobalt mixed oxides,[14] and titanium−zinc oxides[15]) were proven effective for selective capture of H_2S via the formation of metal sulfides, they all suffered from either high regeneration temperatures (>400 °C) or were unable to simultaneously remove H_2S and CO_2. It is noted that similar conclusions have been reached for porous activated carbon, inorganic zeolites, and "molecular basket sorbents"—different classes of materials that suffer significant obstacles to improvement due to the lack of control over their structural features and functionality.[3,16] Recently, the performance of metal−organic frameworks (MOFs) have also been explored, albeit with mixed results.[17−19] Though MOFs have added value in the flexibility with which their structures are designed and modified, they have, thus far, experienced difficulty for this specific application due to the not-so-strong coordinative bonds between the organic linkers and the inorganic clusters, which allows for irreversible bond formation upon exposure to H_2S.[17−19] Finally, it is noted that polymeric-based membranes have shown initial promise for CO_2 and H_2S separation from natural gas streams.[20,21] However, it remains a significant challenge to design suitable polymeric materials for large-scale membrane separation that maintain high H_2S/CH_4 selectivity with high permeability and stability under industrial practical conditions. Although these important classes of solid sorbent materials have all been extensively studied, virtually no work has been undertaken to assess the potential of porous organic polymers (POPs) as stand-alone bulk sorbents for the H_2S removal from natural gas as the main challenge in the natural gas sweetening processes.[3] This is surprising given the fact that POPs are well-known to combine permanent porosity with reasonably high and selective CO_2 capacity, demonstrate fast adsorption kinetics, and are constructed from irreversible, strong bonds (i.e. intrinsic chemical stability), all of which are physicochemical properties that lend support to their potential use as effective sorbent materials for this application.

In this contribution, we report a new porous organic polymer, termed KFUPM-5, that was synthesized via acid catalyzed polycondensation of polar aromatic monomers, melamine and pyrrole, with *p*-formaldehyde serving as the cross-linking agent (Figure 1). The reasoning behind using these monomers was the fact that a basic, nitrogen-rich backbone would afford the resulting polymer with an overwhelming number of adsorption sites for H_2S and CO_2 to interact with. After full structural characterization and assessment of its gas adsorption properties, KFUPM-5 was demonstrated effective in concurrently and selectively separating H_2S and CO_2 from a simulated natural gas stream. Importantly, the findings detailed herein serve to demonstrate the potential of POPs as a viable class of materials for use as separation sorbents in the challenging natural gas sweetening process.

EXPERIMENTAL SECTION

Materials. The optimization conditions for the synthesized polymer and additional characterization details can be found in the Supporting Information (SI), section S1. Melamine (99% purity), pyrrole (99% purity), and ammonium hydroxide solution (28−30% *w*/*w*) were obtained from Alfa Aeser. *p*-Formaldehyde (≥99% purity) was obtained from Fluka. *N*,*N*′-dimethylformamide (DMF; 99% purity), methanol (99.9% purity), and concentrated hydrochloric acid (HCl, 37%) were purchased from MilliporeSigma. All chemicals, unless specified, were used as received without purification with the exception of pyrrole, which was distilled at 145 °C under N_2 flow. For the gas sorption measurements, ultrahigh purity (99.999%) N_2, He, and CH_4 and high purity CO_2 (99.99%) were supplied from AHG Industrial Co. LTD, Dammam, Saudi Arabia. Hydrogen sulfide-based gas mixtures (0.2% H_2S in 99.8% CH_4 *v*/*v* and 0.51% H_2S, 9.99% CO_2, and 89.5% CH_4 *v*/*v*) were also purchased from AHG Industrial Co., Ltd., Dammam, Saudi Arabia.

Structure Characterization. Solid-state ^{13}C nuclear magnetic resonance (NMR) spectroscopy was performed using a Bruker 400 MHz spectrometer at 125.65 MHz and ambient temperature. Four millimeter ZrO_2 rotors were used and cross-polarization magic angle

https://dx.doi.org/10.1021/acsami.0c14259
ACS Appl. Mater. Interfaces XXXX, XXX, XXX−XXX

spinning (14 kHz rate) was applied with a 5 s pulse delay. Fourier transform infrared (FT-IR) spectra were recorded using KBr pellets on a PerkinElmer 16 PC spectrometer from 4000 to 600 cm^{-1}. The resulting signals were identified as br, broad; s, strong; medium; and w, weak. The carbon, hydrogen, and nitrogen content in the material was determined using a PerkinElmer EA-2400 elemental analyzer. Thermogravimetric analysis (TGA) was measured using a TA Instruments Q500 under airflow at a heating rate of 10 °C min^{-1}. Powder X-ray diffraction (PRXD) analysis was performed using a Rigaku MiniFlex II instrument with Cu Kα radiation (λ = 1.541 Å).

Gas Adsorption Measurements. Low-pressure N_2 isotherms were measured using a Quantachrome Quadrasorb Evo at 77 K. The materials were activated before the measurement by degassing at 383 K under high vacuum (10^{-3} Torr). CO_2, CH_4, and N_2 sorption isotherms under static conditions were measured on a Quantachrome Autosorb iQ2 volumetric gas adsorption instrument at 273 and 298 K. The temperatures were controlled during the analysis using a water chiller circulator.

Synthesis of the Porous Organic Polymer, KFUPM-5. Melamine (1.26 g, 10.0 mmol) and *p*-formaldehyde (2.10 g, 70.0 mmol) were added with 50 mL of DMF in a 125 mL round-bottom flask and vigorously stirred at room temperature for 5 min. Pyrrole (2.00 g, 30.0 mmol) was then added into the reaction mixture and continuously stirred for an additional 5 min. HCl (1.00 mL) was then added dropwise, and the flask was sealed with a rubber septum. The reaction mixture was transferred to a preheated oil bath at 90 °C and vigorously stirred for 24 h at a rate of 700 rpm. It is noted that a black solid formed after 5 min of adding all of the reagents. The resulting solid, after 24 h, was washed with 60 mL of methanol followed by sonication for 30 min. The solid was continuously washed with methanol for 3 days (3 × 100 mL per day) under stirring, at which time a clear filtrate solution was obtained. The solid was then immersed in an ammonium hydroxide solution (28−30% *w*/*w*) for 2 h, filtered, washed with 150 mL distilled water and continuously immersed in 150 mL of distilled water for 24 h. Solvent exchange using methanol was carried out for 1 day (3 × 100 mL) with stirring. Finally, the product was dried at 80 °C in an oven for 12 h. The final yield (4.34 g) was 99.5% based on the monomer weights excluding the equivalent amount of water generated as a byproduct of the polymerization. The yield was calculated as follows: % yield = [experimental weight/(total monomers weights−weight of generated H_2O)] × 100. EA: Calculated for $C_{21}H_{21}N_9$: C, 63.14; H, 5.29; N, 31.56; C/N = 2.00. Found: C, 48.24; H, 4.00; N, 23.34; C/N = 2.06. FT-IR (KBr, cm^{-1}): 3406 (br), 3238 (br), 2918 (m), 2850 (w), 1624 (m), 1564 (m), 1466 (w), 1338 (w), 814 (m).

CO_2/N_2 Binary and Ternary Mixed Gas Stream Breakthrough Measurements. Details about the gas adsorption experiments and calculations, breakthrough measurement setup, and the corresponding parameters are provided in the SI, section S5. Typically, KFUPM-5 powder (~1.0 g) was packed into the breakthrough column and activated at 100 °C under vacuum for 24 h. The breakthrough measurements were performed under ambient conditions (room temperature and 1 bar) with a flow rate of 10 sccm of the feed mixture CO_2:N_2 (20:80 *v*/*v*). For wet breakthrough tests, the N_2 gas line was connected to a humidifier, and a continuous wet gas stream was monitored by mass spectrometry detector until saturation achieved (~91% relative humidity, RH). Then dry CO_2 was introduced and mixed with the wet N_2 flow with the same specified flow rate as the dry conditions. The breakthrough capacity of the CO_2 was calculated from the ratio of the downstream and the feed gases. Regeneration of the sample was conducted at room temperature by continuously flowing pure wet N_2 through the column for 5−6 h at 100 °C.

H_2S-Based Binary and Ternary Mixed Gas Stream Breakthrough Measurements. Details about the H_2S breakthrough measurement setup are provided in the SI section S5. The binary breakthrough measurements were performed at room temperature by packing KFUPM-5 powder (~0.5 g) into a fixed bed column (i.d. × l = 2 × 200 mm). Quartz fiber was used at both ends of the column to maintain the polymer inside the column. The binary gas mixture containing 0.2% H_2S and 99.8% CH_4 (*v*/*v*) was passed through the column at a flow rate of 10 sccm. The outlet H_2S gas was monitored by gas chromatography with a thermal conductivity detector. The excess gas was absorbed in a NaOH solution for safety purposes. The breakthrough capacity of H_2S was estimated based on the breakthrough time when the downstream H_2S concentration reached 5 ppm. Regeneration of KFUPM-5 was performed using a N_2 gas flow at 60 °C.

For the ternary mixed gas stream breakthrough measurement, ~0.8 g of KFUPM-5 was packed in a fixed bed column (i.d. × l = 6 mm × 60 cm). The flow rate (10 sccm) of the ternary gas mixture (H_2S = 0.51%, CO_2 = 9.99%, and CH_4 = 89.5%, *v*/*v*) was controlled by mass flow controllers, and the outlet gas was analyzed by an online gas chromatography (Agilent 490 Micro GC). The measurements were performed under ambient conditions (25 °C and 1 bar). Prior to performing the breakthrough measurement, KFUPM-5 was activated by flowing pure N_2 gas at 100 °C for 24 h through the column to remove any adsorbed water or guest molecules.

Computational Methods. Full computational details are provided in the SI, section S4. To reveal the underlying mechanistic processes leading to the adsorption of the gas molecules, the core unit of KFUPM-5, the targeted gas molecules (CO_2 and H_2S), and the polymer−gas complexes were optimized using the Grimme's density functional theory (DFT-D3) method, which takes into consideration the dispersion corrections,[22,23] at the highly parametrized Minnesota approximate exchange-correlation (m06)[24] and the hybrid Becke[25] and Lee[26] (B3LYP) functionals. The starting geometries of the molecules were built on GaussView 5.0 graphical user interface,[27] while the simulations were accomplished on Gaussian 09 software suite,[28] using the 6-311+G* and the 6-311++G** basis sets. Local reactivity sites on the polymer molecules were determined by the condensed Fukui functions calculated using the UCA-FUKUI v.1.0 software via the finite difference approximation method.[29] The Fukui functions (f_k^+, f_k^-, and f_k° representing atomic sites prone to nucleophilic, electrophilic and radical attacks, respectively), therefore, allow us to predict where the most electrophilic and nucleophilic atoms on the molecule are sited and designated as M1 and M2 as presented in the SI, section S4 geometry optimizations were carried out to the minima without imposing symmetry constraints on the potential energy surface. The quantum chemical reactivity descriptors, energy of the highest occupied molecular orbital (E_{HOMO}), energy of the lowest unoccupied molecular orbital (E_{LUMO}), band gap (ΔE), electronegativity (χ), global hardness (η), and dipole moment (μ), were computed following the DFT-Koopman's ionization theorem.[30] Aqueous media simulations were carried out using Tomasi's polarized continuum model with the self-consistent reaction field (PCM-SCRF), and the solvent was chosen as water.[31] Adsorption of the gas molecules on the core unit of KFUPM-5 at the molecular level were simulated following a previously reported model.[32] The counterpoise correction was imposed to account for errors resulting from basis set superposition, BSSE.[33] Energies of adsorption were estimated according to the equation

$$E_{ads} = E_{p/gas} - E_p - E_{gas} - E_{BSSE}$$

where $E_{p/gas}$, E_p, and E_{gas} represents the free energies of the polymer/gas complexes, the isolated core unit of KFUPM-5, and the isolated gas molecules, respectively, while E_{BSSE} represents the counterpoise corrected basis set superposition error. To analyze the real space functions and to characterize the types of interactions, the quantum theory of atoms in molecules (QTAIM) was used according to the Bader's theory[34] using the Multiwfn code.[35] This enables us to characterize the bond critical points (BCPs) in the form of electron density, ρ and the Laplacian of electron density, $\nabla^2\rho$. Lastly, the reduced density gradient, RDG method was used to characterize the nature and strength of the interactions of KFUPM-5 and the targeted gas molecules through the visual analysis of the estimated isosurfaces.

https://dx.doi.org/10.1021/acsami.0c14259
ACS Appl. Mater. Interfaces XXXX, XXX, XXX−XXX

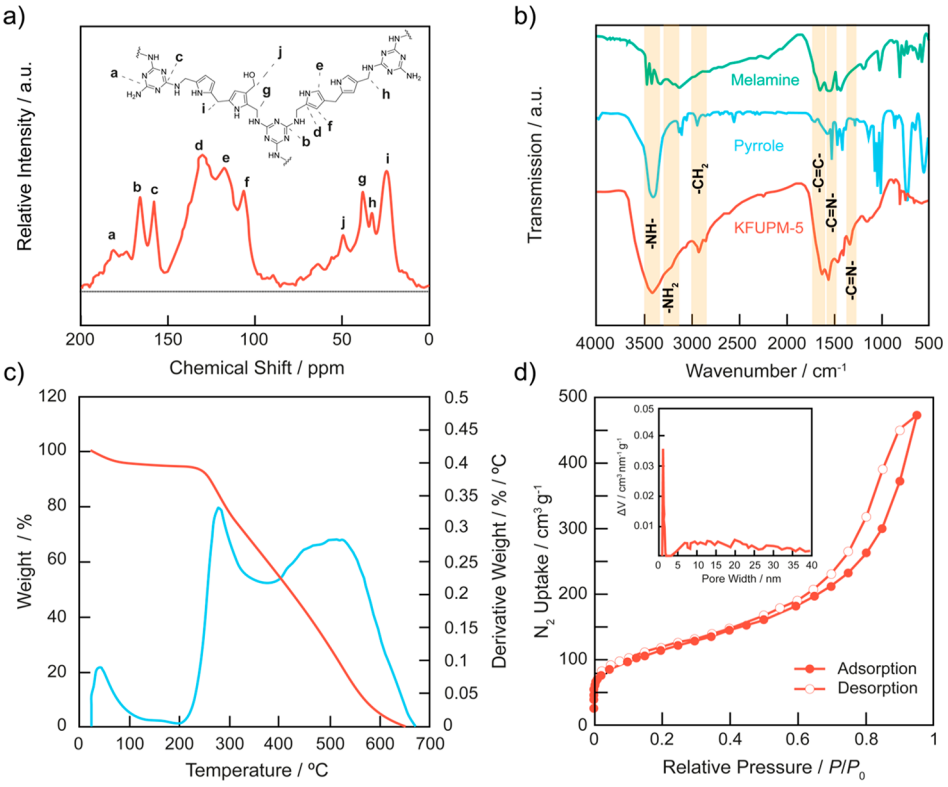

Figure 2. Structural characterization of KFUPM-5. (a) CP-MAS ^{13}C NMR spectrum of KFUPM-5, with the core structure of the polymer provided in the inset for corresponding peak identification and assignment. (b) FT-IR spectrum of KFUPM-5 (red) in comparison to the spectra for the pure monomers, melamine (green), and pyrrole (blue). Those absorption bands directly related to the identification of the characteristic functional groups in KFUPM-5 are highlighted in light orange. (c) TG curve (red) with the first derivative of the TG curve (blue; Δ weight loss/temperature) demonstrating the material's thermal robustness. (d) N_2 isotherm at 77 K with the pore size distribution provided in the inset. Filled and open circles represent the adsorption and desorption branches, respectively. The connecting lines serve as guides for the eye.

RESULTS AND DISCUSSION

Synthesis Strategy for Realizing the Novel Porous Organic Polymer, KFUPM-5. In our efforts to realize practical sorbents for addressing energy-intensive gas separations, we targeted the synthesis of a nitrogen-rich porous organic polymer from inexpensive aromatic amines.[36,37] The choice to use the polar aromatic amines, melamine and pyrrole, as monomers was made given their ability to induce strong interactions upon physical adsorption of CO_2 and other potentially polarizable gas molecules like H_2S.[38−41] We employed an acid-catalyzed polycondensation reaction with *p*-formaldehyde serving as a cross-linking agent.[36,37,41] The most effective synthetic conditions for producing the novel polymer, termed KFUPM-5, in its final, optimized form were DMF as the solvent, conc. HCl as the acid catalyst, and a melmine:pyrrole molar ratio of 1:3 (Figure 1; SI, section S1). It is noted that KFUPM-5 could be synthesized by different synthetic conditions, but those realized products lacked optimized surface areas and/or gas uptake (SI, section S2). After synthesis, KFUPM-5 was subsequently purified by washing with methanol and water to remove any unreacted starting materials or oligomeric byproducts. Finally, to yield a guest-free porous material, KFUPM-5 was activated at 80 °C in an oven for 24 h.

Structural Characterization, Architectural Robustness, and Permanent Porosity. Powder X-ray diffraction analysis demonstrated that KFUPM-5 was amorphous. Therefore, structural understanding of KFUPM-5 (i.e., incorporation of monomers and their corresponding connectivity within the structure) resulted from a combination of CP-MAS ^{13}C NMR and FT-IR spectroscopies along with elemental analysis for chemical formulation (Figure 2a and b). The ^{13}C NMR spectrum revealed several important resonance signals (Figure 2a). Most importantly, confirmation of cross-linked melamine and pyrrole monomers was achieved by identifying the following characteristic peaks of the methylene ($-CH_2-$) unit: (i) δ = 27 ppm was assigned to methylene when linking two pyrrole monomers together; (ii) δ = 40 ppm was established to be a methylene unit bridging the α-carbon of pyrrole with − NH of melamine; and (iii) δ = 37 ppm was identified as the methylene connecting the β-carbon of pyrrole with −NH of melamine. An additional signal at δ = 58 ppm was attributed to the chemical shift of the carbon atom in the terminal $-CH_2OH$ group that is derived from *p*-formaldehyde.

Other important signals identified are as follows: (i) The broad peaks at δ = 132 and 108 ppm were the pyrrole α-carbon and β-carbon, respectively, when the pyrrole unit is connected from the α position; (ii) δ = 118 ppm was determined to be a pyrrole unit when connected from the β-carbon; (iii) the sharp resonance signal centered at δ = 180 ppm is the melamine triazenyl carbon with free amine units; and (iv) δ = 160 ppm is the characteristic chemical shift for the triazenyl ring of the melamine monomer when fully connected with pyrrole units. Taken together, the observed and assigned resonance signals provide conclusive evidence for the incorporation of both monomers and their subsequent connectivity within the structure.

https://dx.doi.org/10.1021/acsami.0c14259
ACS Appl. Mater. Interfaces XXXX, XXX, XXX−XXX

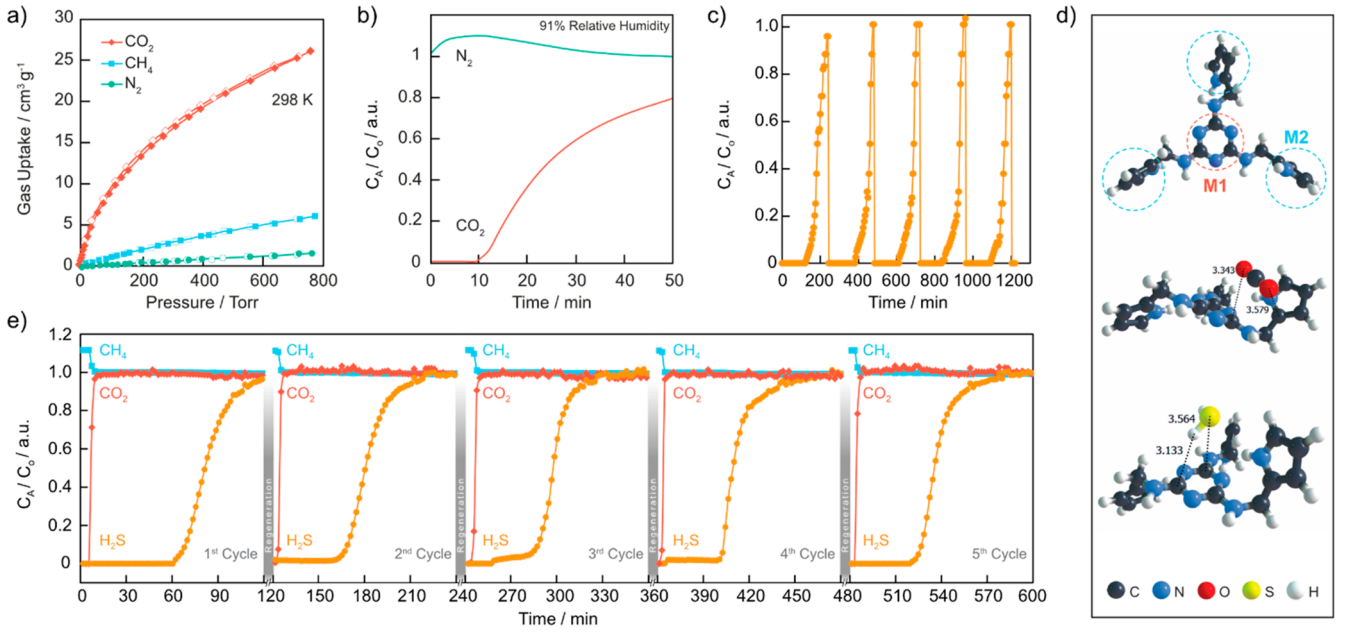

Figure 3. Gas separation performance of KFUPM-5: (a) CO_2 (red diamonds), CH_4 (blue squares), and N_2 (green circles) adsorption properties of KFUPM-5 at 298 K. Open and filled symbols represent adsorption and desorption branches, respectively. The connecting lines serve as guides for the eye. (b) Dynamic breakthrough measurement demonstrating the ability of KFUPM-5 to effectively separate a ternary gas mixture of 20% CO_2 (red) and 80% N_2 (green) v/v under wet conditions (91% RH) at 298 K and 1 bar. (c) Dynamic breakthrough measurements using a binary gas mixture containing 0.2% v/v H_2S in methane. The breakthrough curves for KFUPM-5 exhibit a near-perfect recyclability over 5 consecutive cycles. (d) Optimized molecular geometry of the core unit of KFUPM-5. Calculated interaction distances of CO_2 and H_2S with the core unit of KFUPM-5 (middle and bottom). Atom colors: C, gray; N, dark blue; O, red; S, yellow; and H, light blue. (e) Dynamic breakthrough measurements demonstrating the effectiveness of KFUPM-5 to concurrently and selectively capture CO_2 and H_2S from a complex, ternary gas mixture containing H_2S (orange circles; 0.51% v/v), CO_2 (red diamonds; 9.99% v/v), and CH_4 (blue squares; 89.5% v/v) at 298 K and 1 bar.

Additional support for structural elucidation of KFUPM-5 was then provided by FT-IR spectroscopy (Figure 2b). Accordingly, the FT-IR spectrum for KFUPM-5 exhibited a broad absorption band at 3400 cm^{-1}, which is characteristic of the ν_{N-H} stretching frequency for both pyrrole and melamine. At 2900 cm^{-1}, a new absorption band is observed for KFUPM-5 and is assigned to the ν_{C-H} stretching frequency of the methylene cross-linking unit. This absorption band is not observed in either of the FT-IR spectra measured for the pure monomers. Direct evidence for the incorporation of melamine is provided by two strong absorption bands at 1560 and 1340 cm^{-1}, which are attributed to a $\nu_{C=N}$ stretching frequency and ring breathing mode of vibration, respectively. Finally, at 1640 cm^{-1}, the $\nu_{C=C}$ stretching frequency for pyrrole was observed in both the spectrum of KFUPM-5 and pure pyrrole, thereby providing further support for the incorporation of pyrrole within the structure.

To formulate KFUPM-5, elemental analysis was performed. It is important to note that actual chemical formulation is notoriously difficult to perform on materials similar to KFUPM-5 because of the irregularity of the polymer structure as well as incomplete combustion that leads to trapped adsorbate molecules (i.e., gases and water vapors).[39,42,43] Despite this, the experimentally derived C/N ratio of the activated KFUPM-5 satisfactorily agrees with the theoretical C/N ratio calculated from the precursor monomers: C = 63.14 (48.24), H = 5.29 (4.00), N = 31.56 (23.34), and C/N = 2.00 (2.06) for the theoretical (experimental) values, respectively.

Provided the structure, our attention turned to assessing the polymer's thermal stability and permanent porosity (Figure 2c and d). Under air flow, the thermal gravimetric (TG) profile of KFUPM-5 displayed a gradual weight loss after 270 °C, indicating a relatively high thermal stability for the material. When taking the first derivative of the TG curve (Δ weight loss/temperature), the decomposition of specific chemical bonds can be identified from the peak areas. The small peak present before 200 °C is assigned to water molecules trapped within the pores, whereas the second sharp peak at 270 °C reflects the thermal decomposition of the melamine-methylene cross-linkage ($NH-CH_2-$). The permanent porosity of KFUPM-5 was then established by measuring a N_2 isotherm at 77 K. As expected, the N_2 isotherm displays a sharp uptake at low relative pressure ($P/P_0 < 0.001$) indicating the presence of pores within the microporous size regime. A steep rise in the N_2 uptake at higher relative pressures ($P/P_0 > 0.5$) points to the likelihood of capillary condensation of N_2 molecules within the structure. Indeed, the presence of both micro- and mesopores within KFUPM-5 was confirmed by pore size distribution analysis (Figure 2d inset). Upon desorption, hysteresis was observed indicating elastic deformation and/or swelling of the polymer; phenomena that are present in many similarly related materials.[44] The Brunauer–Emmett–Teller (BET) surface area of KFUPM-5 was calculated to be 400 $m^2 g^{-1}$.

Thermodynamic Gas Adsorption Properties. Upon proving permanent porosity, our attention turned toward gleaning insight into the material's ability to capture CO_2 as opposed to other gases present in relevant natural gas streams. Accordingly, thermodynamic CO_2, N_2, and CH_4 adsorption isotherms were measured at 273 and 298 K (Figure 3a). All isotherms exhibit reversible adsorption and desorption, indicating the physical adsorption (no chemical bond formation) of the respective gas with the polymer backbone. At 760 Torr, KFUPM-5 reached a total CO_2 uptake capacity of

https://dx.doi.org/10.1021/acsami.0c14259
ACS Appl. Mater. Interfaces XXXX, XXX, XXX–XXX

Table 1. Dynamic H_2S Capacity for KFUPM-5 at 298 K and 1 Bar in Comparison with Other Representative Sorbents

			H_2S/CH_4[a]		$H_2S/CO_2/CH_4$	
material	class	SA_{BET} ($m^2\ g^{-1}$)	dynamic H_2S capacity ($cm^3\ g^{-1}$)	dynamic CO_2 capacity ($cm^3\ g^{-1}$)	dynamic H_2S capacity ($cm^3\ g^{-1}$)	ref
KFUPM-5	POP	400	4.88[a]	7	4.1[b]	this work
(fSi-PEI800-40)	polyamine/silica	43.5	26.8	30	1.41	6
PA(30)/SAB-15	polyamine/silica	–	2.07[c]	–	0.07[c]	59
PEI(30)/SAB-15	polyamine/silica	–	3.24[c]	–	0.98[c]	59
SAB-16/TBAPS	amine/silica	354	2.24	28	2.24	60
MIL-101 (Cr)	MOF	3203	–	–	8.96	61
Mg-MOF-74	MOF	1244	5.3	–	–	61
Ga-soc-MOF-1a	MOF	1350	–	2.5	20	62
AlFFIVE-1-Ni	MOF	–	50.4	29.1	30.2	4

[a]Composition: 0.2% H_2S in CH_4 (v/v). [b]Composition: H_2S (0.51% v/v), CO_2 (9.99% v/v), and CH_4 (89.5% v/v). [c]Composition: H_2S (500 ppm) and CO_2 (10% v/v) in N_2. Those data that are not reported are identified as —.

39.0 and 26.0 $cm^3\ g^{-1}$ at 273 and 298 K, respectively. Though modest in value, the CO_2 capacities were significantly higher than those measured for CH_4 (10.1 and 6.0 $cm^3\ g^{-1}$ at 273 and 298 K, respectively) and N_2 (1.8 and 1.6 $cm^3\ g^{-1}$ at 273 and 298 K, respectively) at 760 Torr. These results for CO_2 capacity are comparable to those reported for other porous organic materials, such as covalent organic frameworks (COFs; COF-5, 29.9 $cm^3\ g^{-1}$; COF-8, 32.0 $cm^3\ g^{-1}$; and COF-10, 27.0 $cm^3\ g^{-1}$)[45] and porous organic polymers (PA-M, 9.6 $cm^3\ g^{-1}$; CMP-1, 29.6 $cm^3\ g^{-1}$; PPN-6-CH_2Cl, 28.6 $cm^3\ g^{-1}$; PoBCs, 31.4 $cm^3\ g^{-1}$; KFUPM-1, 36.8 $cm^3\ g^{-1}$; NUT-1, 36 $cm^3\ g^{-1}$; and CPC-550, 129.9 $cm^3\ g^{-1}$).[36,46−52]

As shown in Figure 3a, the initial slope of the CO_2 isotherm was much steeper than those observed for CH_4 or N_2, which qualitatively reflects a higher affinity of KFUPM-5 toward CO_2. Coverage-dependent isosteric heats of adsorption were calculated for CO_2, CH_4, and N_2 by fitting the respective isotherms at 273 and 298 K with a viral-type equation. As such, the zero-coverage heat of adsorption was significantly higher for CO_2 (36 kJ mol^{-1}) when compared with CH_4 and N_2 (22 and 17 kJ mol^{-1}, respectively) (SI, section S2). Prior to measuring KFUPM-5's dynamic separation properties, we sought to also calculate the thermodynamic adsorption selectivity via ideal adsorbed solution theory (IAST). For CO_2/N_2 (v/v = 20:80) and CO_2/CH_4 (v/v = 10:90), the IAST selectivities at 298 K were 71 and 15, respectively (SI, section S2).

Given the effectiveness of KFUPM-5 for removing CO_2 from these mixed gas streams, we then sought to assess the material's potential for the more challenging separation behind natural gas sweetening. The main impurities in natural gas are CO_2 and H_2S, whose presence cause severe corrosion and considerable energy consumption to remove.[52−58] Following a similar breakthrough protocol, KFUPM-5 was subjected to a simple binary gas mixture of 0.2% H_2S in CH_4 (v/v), in which the material was able to retain H_2S within its structure for >120 min resulting in a dynamic capacity of 4.9 $cm^3\ g^{-1}$ (Figure 3c). To assess KFUPM-5's performance stability and recyclability toward H_2S separation, a multicyclic (five cycles) H_2S/CH_4 breakthrough experiment was performed. Accordingly, it was observed that the H_2S retention time (>120 min) remained unchanged over the course of five consecutive adsorption−desorption cycles with regeneration of the material occurring between each cycle by simply flowing N_2 at 60 °C (Figure 3c).

Though a promising initial result, the most important breakthrough measurement is one in which H_2S and CO_2 are present together in a mixed gas stream as the effect of competitive adsorption on the material's overall performance is a significant variable to consider. Accordingly, a fourth breakthrough experiment was conducted whereby KFUPM-5 was subjected to a complex ternary gas mixture containing H_2S (0.51% v/v), CO_2 (9.99% v/v), and CH_4 (89.5% v/v). As it clearly shows in Figure 3e, CH_4 passes through the material almost instantly, while CO_2 and H_2S are captured concurrently. From this measurement, dynamic uptake capacities were calculated to be 7 and 4.1 $cm^3\ g^{-1}$ for CO_2 and H_2S, respectively. The presence of CO_2 in the mixed gas stream had little to no effect on the dynamic capacity of H_2S. It is important to point out that these dynamic capacities are higher than other reported polymeric-based sorbents, all of which displayed a dramatic drop in H_2S dynamic capacity when CO_2 was present in the gas mixture. This is because of the adsorption of CO_2 and H_2S in KFUPM-5 occurs via a physisorption mechanism whereas for the others, chemisorption occurs as a result of the presence of aliphatic amines (Table 1).

Following this exciting result, we once again performed a recycling measurement whereby KFUPM-5 was subjected to five consecutive breakthrough measurements with regeneration occurring between each cycle by flowing N_2 at 100 °C. Although KFUPM-5 experienced a ∼20% decrease in capacity after the first cycle, there was no subsequent drop in performance between the second and fifth cycles (Figure 3e). Comparison of the CP-MAS ^{13}C NMR spectra before and after the H_2S breakthrough measurements confirmed the fact that the structure of KFUPM-5 was retained (Figure S27).

When turning again to DFT calculations to glean deeper insight into the interactions between the adsorbent and H_2S, we find that KFUPM-5 has a slightly higher selectivity toward CO_2 over H_2S, which supports the experimental breakthrough results (SI, section S4). The calculated interaction of H_2S and CO_2 with the core unit of KFUPM-5 were, on average, stronger for CO_2 than H_2S (Figure 3d, SI, section S4). When taken together, these results demonstrate the extraordinary potential of KFUPM-5 for the concurrent and selective removal of H_2S and CO_2 from natural gas streams.

https://dx.doi.org/10.1021/acsami.0c14259
ACS Appl. Mater. Interfaces XXXX, XXX, XXX−XXX

Finally, we evaluated the energy of adsorption of the gas molecules on the KFUPM-5 core unit in vacuum and in aqueous media, and the results at all levels of theory are presented in SI, section S4. The results revealed that the KFUPM-5 core unit is selective toward CO_2 over H_2S because of the presence of stronger van der Waals interactions. These interactions were further enhanced in aqueous media leading to higher adsorption capacity as predicted by quantum chemical reactivity descriptor analyses and in agreement with experimental data.

CONCLUSION

We have successfully employed an acid-catalyzed polycondensation reaction to produce a new microporous organic polymer, termed KFUPM-5. The distinct structural features of KFUPM-5, including its permanent porosity (BET = 400 $m^2 g^{-1}$), polar backbone as a result of the aromatic amine monomers chosen, and selective CO_2 capture properties, afforded an effective adsorbent for concurrently removing acid gas impurities (H_2S and CO_2) from complex natural gas streams. Although porous organic polymers have been reported for the selective capture of CO_2 from gas mixtures under both dry and wet conditions, this original work represents an example of moving beyond CO_2 flue gas scrubbing by such materials to the more challenging separation behind natural gas sweetening. Furthermore, it is noted that KFUPM-5 is capable of being rapidly and facilely scaled up for pilot testing. Future work will be dedicated to increasing the dynamic uptake capacities of both H_2S and CO_2 while at the same time demonstrating long-term stability under industrially prescribed conditions without loss of separation performance.

ASSOCIATED CONTENT

Supporting Information

The Supporting Information is available free of charge at https://pubs.acs.org/doi/10.1021/acsami.0c14259.

KFUPM-5 synthesis and characterization, as well as the experimental conditions (PDF)

AUTHOR INFORMATION

Corresponding Author

Othman Charles S. Al Hamouz − *Department of Chemistry, King Fahd University of Petroleum and Minerals (KFUPM), Dhahran 31261, Saudi Arabia*; Email: othmanc@kfupm.edu.sa

Authors

Mahmoud M. Abdelnaby − *Department of Chemistry and King Abdulaziz City for Science and Technology, Technology Innovation Center on Carbon Capture and Sequestration (KACST-TIC on CCS), King Fahd University of Petroleum and Minerals (KFUPM), Dhahran 31261, Saudi Arabia*

Kyle E. Cordova − *Materials Discovery Research Unit, Research and Development Pillar, Royal Scientific Society, Amman 11941, Jordan*; orcid.org/0000-0002-4988-0497

Ismail Abdulazeez − *Department of Chemistry, King Fahd University of Petroleum and Minerals (KFUPM), Dhahran 31261, Saudi Arabia*

Ahmed M. Alloush − *Department of Chemistry and King Abdulaziz City for Science and Technology, Technology Innovation Center on Carbon Capture and Sequestration (KACST-TIC on CCS), King Fahd University of Petroleum and Minerals (KFUPM), Dhahran 31261, Saudi Arabia*

Bassem A. Al-Maythalony − *King Abdulaziz City for Science and Technology, Technology Innovation Center on Carbon Capture and Sequestration (KACST-TIC on CCS), King Fahd University of Petroleum and Minerals (KFUPM), Dhahran 31261, Saudi Arabia*; orcid.org/0000-0003-3104-2214

Youcef Mankour − *Process & Control Systems Department, Upstream Engineering Division, Gas Processing Unit, Saudi Aramco, Dhahran 31311, Saudi Arabia*

Khalid Alhooshani − *Department of Chemistry, King Fahd University of Petroleum and Minerals (KFUPM), Dhahran 31261, Saudi Arabia*; orcid.org/0000-0002-6119-668X

Tawfik A. Saleh − *Department of Chemistry, King Fahd University of Petroleum and Minerals (KFUPM), Dhahran 31261, Saudi Arabia*

Complete contact information is available at: https://pubs.acs.org/10.1021/acsami.0c14259

Funding

We acknowledge financial support for this project provided by Saudi Aramco (Project No. 6510895769).

Notes

The authors declare no competing financial interest.

ACKNOWLEDGMENTS

We are grateful to KFUPM and CENT for use of their facilities. We appreciate Dr. Mostafa Zeama and Mr. Mohamed Sanhoob (CENT) for their support with the IAST calculations and the breakthrough experiments, respectively.

REFERENCES

(1) He, Y.; Zhou, W.; Qian, G.; Chen, B. Methane storage in metal−organic frameworks. *Chem. Soc. Rev.* **2014**, *43* (16), 5657−5678.

(2) Mohideen, M. I. H.; Pillai, R. S.; Adil, K.; Bhatt, P. M.; Belmabkhout, Y.; Shkurenko, A.; Maurin, G.; Eddaoudi, M. A fine-tuned MOF for gas and vapor separation: A multipurpose adsorbent for acid gas removal, dehydration, and BTX Sieving. *Chem.* **2017**, *3* (5), 822−833.

(3) Shah, M. S.; Tsapatsis, M.; Siepmann, J. I. Hydrogen Sulfide Capture: From Absorption in Polar Liquids to Oxide, Zeolite, and Metal-Organic Framework Adsorbents and Membranes. *Chem. Rev.* **2017**, *117* (14), 9755−9803.

(4) Belmabkhout, Y.; Bhatt, P. M.; Adil, K.; Pillai, R. S.; Cadiau, A.; Shkurenko, A.; Maurin, G.; Liu, G.; Koros, W. J.; Eddaoudi, M. Natural gas upgrading using a fluorinated MOF with tuned H_2S and CO_2 adsorption selectivity. *Nat. Energy* **2018**, *3* (12), 1059−1066.

(5) Belmabkhout, Y.; Heymans, N.; De Weireld, G.; Sayari, A. Simultaneous adsorption of H_2S and CO_2 on triamine-grafted pore-expanded mesoporous MCM-41 silica. *Energy Fuels* **2011**, *25* (3), 1310−1315.

(6) Yoosuk, B.; Wongsanga, T.; Prasassarakich, P. CO_2 and H_2S binary sorption on polyamine modified fumed silica. *Fuel* **2016**, *168*, 47−53.

(7) Tsai, J.-H.; Jeng, F.-T.; Chiang, H.-L. Removal of H_2S from Exhaust Gas by Use of Alkaline Activated Carbon. *Adsorption* **2001**, *7* (4), 357−366.

(8) Adib, F.; Bagreev, A.; Bandosz, T. J. Analysis of the Relationship between H_2S Removal Capacity and Surface Properties of Unimpregnated Activated Carbons. *Environ. Sci. Technol.* **2000**, *34* (4), 686−692.

(9) Sayari, A.; Belmabkhout, Y.; Serna-Guerrero, R. Flue gas treatment via CO_2 adsorption. *Chem. Eng. J.* **2011**, *171* (3), 760−774.

(10) Britt, D.; Tranchemontagne, D.; Yaghi, O. M. Metal-organic frameworks with high capacity and selectivity for harmful gases. *Proc. Natl. Acad. Sci. U. S. A.* **2008**, *105* (33), 11623−11627.
(11) Haszeldine, R. S. Carbon capture and storage: how green can black be? *Science* **2009**, *325* (5948), 1647−1652.
(12) Davidson, J. M.; Lawrie, C. H.; Sohail, K. Kinetics of the absorption of hydrogen sulfide by high purity and doped high surface area zinc oxide. *Ind. Eng. Chem. Res.* **1995**, *34* (9), 2981−2989.
(13) Yamamoto, T.; Tayakout-Fayolle, M.; Geantet, C. Gas-phase removal of hydrogen sulfide using iron oxyhydroxide at low temperature: Measurement of breakthrough curve and modeling of sulfidation mechanism. *Chem. Eng. J.* **2015**, *262*, 702−709.
(14) Baird, T.; Campbell, K. C.; Holliman, P. J.; Hoyle, R.; Noble, G.; Stirling, D.; Williams, B. P. Mixed cobalt−iron oxide absorbents for low-temperature gas desulfurisation. *J. Mater. Chem.* **2003**, *13* (9), 2341−2347.
(15) Polychronopoulou, K.; Fierro, J. L. G.; Efstathiou, A. M. Novel Zn−Ti-based mixed metal oxides for low-temperature adsorption of H_2S from industrial gas streams. *Appl. Catal., B* **2005**, *57* (2), 125−137.
(16) Ma, X.; Wang, X.; Song, C. Molecular basket" sorbents for separation of CO_2 and H_2S from various gas streams. *J. Am. Chem. Soc.* **2009**, *131* (16), 5777−5783.
(17) Martinez-Ahumada, E.; Lopez-Olvera, A.; Jancik, V.; Sanchez-Bautista, J. E.; Gonzalez-Zamora, E.; Martis, V.; Williams, D. R.; Ibarra, I. A. MOF materials for the capture of highly toxic H_2S and SO_2. *Organometallics* **2020**, *39* (7), 883−915.
(18) Rieth, A. J.; Wright, A. M.; Dincă, M. Kinetic stability of metal−organic frameworks for corrosive and coordinating gas capture. *Nat. Rev. Mater.* **2019**, *4* (11), 708−725.
(19) Barea, E.; Montoro, C.; Navarro, J. A. Toxic gas removal−metal−organic frameworks for the capture and degradation of toxic gases and vapours. *Chem. Soc. Rev.* **2014**, *43* (16), 5419−5430.
(20) Yi, S.; Ghanem, B.; Liu, Y.; Pinnau, I.; Koros, W. J. Ultraselective glassy polymer membranes with unprecedented performance for energy-efficient sour gas separation. *Sci. Adv.* **2019**, *5* (5), eaaw5459.
(21) Liu, G.; Chernikova, V.; Liu, Y.; Zhang, K.; Belmabkhout, Y.; Shekhah, O.; Zhang, C.; Yi, S.; Eddaoudi, M.; Koros, W. J. Mixed matrix formulations with MOF molecular sieving for key energy-intensive separations. *Nat. Mater.* **2018**, *17* (3), 283−289.
(22) Grimme, S.; Antony, J.; Ehrlich, S.; Krieg, H. A consistent and accurate ab initio parametrization of density functional dispersion correction (DFT-D) for the 94 elements H-Pu. *J. Chem. Phys.* **2010**, *132* (15), 154104.
(23) Grimme, S.; Ehrlich, S.; Goerigk, L. Effect of the damping function in dispersion corrected density functional theory. *J. Comput. Chem.* **2011**, *32* (7), 1456−1465.
(24) Zhao, Y.; Truhlar, D. G. The M06 suite of density functionals for main group thermochemistry, thermochemical kinetics, noncovalent interactions, excited states, and transition elements: two new functionals and systematic testing of four M06-class functionals and 12 other functionals. *Theor. Chem. Acc.* **2008**, *120* (1), 215−241.
(25) Becke, A. D. Density-functional exchange-energy approximation with correct asymptotic behavior. *Phys. Rev. A: At., Mol., Opt. Phys.* **1988**, *38* (6), 3098−3100.
(26) Lee, C.; Yang, W.; Parr, R. G. Development of the Colle-Salvetti correlation-energy formula into a functional of the electron density. *Phys. Rev. B: Condens. Matter Mater. Phys.* **1988**, *37* (2), 785−789.
(27) Dennington, R. K. T; Millam, J. *GaussView*, version 5; Semichem, Inc.: Shawnee Mission, KS, 2009.
(28) Frisch, M. J.; Trucks, G. W.; Schlegel, H. B.; Scuseria, G. E.; Robb, M. A.; Cheeseman, J. R.; Scalmani, G.; Barone, V.; Mennucci, B.; Petersson, G. A., et al. *Gaussian 09*, revision B.01; Wallingford, CT, 2009.
(29) Sánchez-Márquez, J.; Zorrilla, D.; Sánchez-Coronilla, A.; de los Santos, D. M.; Navas, J.; Fernández-Lorenzo, C.; Alcántara, R.; Martín-Calleja, J. Introducing "UCA-FUKUI" software: reactivity-index calculations. *J. Mol. Model.* **2014**, *20* (11), 2492.
(30) Luo, J.; Xue, Z. Q.; Liu, W. M.; Wu, J. L.; Yang, Z. Q. Koopmans' Theorem for Large Molecular Systems within Density Functional Theory. *J. Phys. Chem. A* **2006**, *110* (43), 12005−12009.
(31) Tomasi, J.; Mennucci, B.; Cammi, R. Quantum Mechanical Continuum Solvation Models. *Chem. Rev.* **2005**, *105*, 2999−3093.
(32) Ullah, R.; Patel, H.; Aparicio, S.; Yavuz, C. T.; Atilhan, M. A combined experimental and theoretical study on gas adsorption performance of amine and amide porous polymers. *Microporous Mesoporous Mater.* **2019**, *279*, 61−72.
(33) Sordo, J. A.; Chin, S.; Sordo, T. L. On the counterpoise correction for the basis set superposition error in large systems. *Theor. Chim. Acta.* **1988**, *74* (2), 101−110.
(34) Bader, R. F. W. *Atoms in Molecules: A Quantum Theory*; Clarendon Press, 1994.
(35) Lu, T.; Chen, F. Multiwfn: A multifunctional wavefunction analyzer. *J. Comput. Chem.* **2012**, *33* (5), 580−592.
(36) Abdelnaby, M. M.; Alloush, A. M.; Qasem, N. A. A.; Al-Maythalony, B. A.; Mansour, R. B.; Cordova, K. E.; Al Hamouz, O. C. S. Carbon dioxide capture in the presence of water by an amine-based crosslinked porous polymer. *J. Mater. Chem. A* **2018**, *6* (15), 6455−6462.
(37) Abdelnaby, M. M.; Qasem, N. A. A.; Al-Maythalony, B. A.; Cordova, K. E.; Al Hamouz, O. C. S. A microporous organic copolymer for selective CO_2 capture under humid conditions. *ACS Sustainable Chem. Eng.* **2019**, *7* (16), 13941−13948.
(38) Chang, Z.; Zhang, D.-S.; Chen, Q.; Bu, X.-H. Microporous organic polymers for gas storage and separation applications. *Phys. Chem. Chem. Phys.* **2013**, *15* (15), 5430−5442.
(39) Luo, Y.; Li, B.; Wang, W.; Wu, K.; Tan, B. Hypercrosslinked aromatic heterocyclic microporous polymers: a new class of highly selective CO_2 capturing materials. *Adv. Mater.* **2012**, *24* (42), 5703−5707.
(40) Hu, L.; Ni, H.; Chen, X.; Wang, L.; Wei, Y.; Jiang, T.; Lü, Y.; Lu, X.; Ye, P. Hypercrosslinked polymers incorporated with imidazolium salts for enhancing CO_2 capture. *Polym. Eng. Sci.* **2016**, *56* (5), 573−582.
(41) Dawson, R.; Adams, D. J.; Cooper, A. I. Chemical tuning of CO_2 sorption in robust nanoporous organic polymers. *Chem. Sci.* **2011**, *2* (6), 1173−1177.
(42) Ren, S.; Bojdys, M. J.; Dawson, R.; Laybourn, A.; Khimyak, Y. Z.; Adams, D. J.; Cooper, A. I. Porous, fluorescent, covalent triazine-based frameworks via room-temperature and microwave-assisted synthesis. *Adv. Mater.* **2012**, *24* (17), 2357−2361.
(43) Xu, Y.; Chen, L.; Guo, Z.; Nagai, A.; Jiang, D. Light-emitting conjugated polymers with microporous network architecture: interweaving scaffold promotes electronic conjugation, facilitates exciton migration, and improves luminescence. *J. Am. Chem. Soc.* **2011**, *133* (44), 17622−17625.
(44) Weber, J.; Antonietti, M.; Thomas, A. Microporous networks of high-performance polymers: Elastic deformations and gas sorption properties. *Macromolecules* **2008**, *41* (8), 2880−2885.
(45) Furukawa, H.; Yaghi, O. M. Storage of hydrogen, methane, and carbon dioxide in highly porous covalent organic frameworks for clean energy applications. *J. Am. Chem. Soc.* **2009**, *131* (25), 8875−8883.
(46) Mane, S.; Gao, Z.-Y.; Li, Y.-X.; Xue, D.-M.; Liu, X.-Q.; Sun, L.-B. Fabrication of microporous polymers for selective CO_2 capture: the significant role of crosslinking and crosslinker length. *J. Mater. Chem. A* **2017**, *5* (44), 23310−23318.
(47) Dawson, R.; Stöckel, E.; Holst, J. R.; Adams, D. J.; Cooper, A. I. Microporous organic polymers for carbon dioxide capture. *Energy Environ. Sci.* **2011**, *4* (10), 4239−4245.
(48) Lu, W.; Sculley, J. P.; Yuan, D.; Krishna, R.; Wei, Z.; Zhou, H. C. Polyamine-tethered porous polymer networks for carbon dioxide capture from flue gas. *Angew. Chem., Int. Ed.* **2012**, *51* (30), 7480−7484.
(49) Senthilkumaran, M.; Saravanan, C.; Sethuraman, V.; Puthiaraj, P.; Muthu Mareeswaran, P. Nitrogen-rich polyaminal porous network

https://dx.doi.org/10.1021/acsami.0c14259
ACS Appl. Mater. Interfaces XXXX, XXX, XXX−XXX

for CO_2 uptake studies and preparation of carbonized materials. *Eur. Polym. J.* **2020**, *124*, 109477.
(50) Qi, S.-C.; Yu, G.-X.; Xue, D.-M.; Liu, X.; Liu, X.-Q.; Sun, L.-B. Rigid supramolecular structures based on flexible covalent bonds: A fabrication mechanism of porous organic polymers and their CO_2 capture properties. *Chem. Eng. J.* **2020**, *385*, 123978.
(51) Soubeyrand-Lenoir, E.; Vagner, C.; Yoon, J. W.; Bazin, P.; Ragon, F.; Hwang, Y. K.; Serre, C.; Chang, J.-S.; Llewellyn, P. L. How water fosters a remarkable 5-fold increase in low-pressure CO_2 uptake within mesoporous MIL-100 (Fe). *J. Am. Chem. Soc.* **2012**, *134* (24), 10174−10181.
(52) Ashourirad, B.; Sekizkardes, A. K.; Altarawneh, S.; El-Kaderi, H. M. Exceptional Gas Adsorption Properties by Nitrogen-Doped Porous Carbons Derived from Benzimidazole-Linked Polymers. *Chem. Mater.* **2015**, *27* (4), 1349−1358.
(53) Yu, J.; Zhai, Y.; Chuang, S. S. Water enhancement in CO_2 capture by amines: an insight into CO_2−H_2O interactions on amine films and sorbents. *Ind. Eng. Chem. Res.* **2018**, *57* (11), 4052−4062.
(54) Nguyen, N. T.; Lo, T. N.; Kim, J.; Nguyen, H. T.; Le, T. B.; Cordova, K. E.; Furukawa, H. Mixed-metal zeolitic imidazolate frameworks and their selective capture of wet carbon dioxide over methane. *Inorg. Chem.* **2016**, *55* (12), 6201−6207.
(55) Wang, K.; Huang, H.; Liu, D.; Wang, C.; Li, J.; Zhong, C. Covalent triazine-based frameworks with ultramicropores and high nitrogen contents for highly selective CO_2 capture. *Environ. Sci. Technol.* **2016**, *50* (9), 4869−4876.
(56) Ma, Y.-X.; Li, Z.-J.; Wei, L.; Ding, S.-Y.; Zhang, Y.-B.; Wang, W. A dynamic three-dimensional covalent organic framework. *J. Am. Chem. Soc.* **2017**, *139* (14), 4995−4998.
(57) Zhao, S.; Yi, H.; Tang, X.; Jiang, S.; Gao, F.; Zhang, B.; Zuo, Y.; Wang, Z. The hydrolysis of carbonyl sulfide at low temperature: A review. *Sci. World J.* **2013**, *2013*, 739501.
(58) Qian, Z.; Xu, L.-B.; Li, Z.-H.; Li, H.; Guo, K. Selective absorption of H_2S from a gas mixture with CO_2 by aqueous N-methyldiethanolamine in a rotating packed bed. *Ind. Eng. Chem. Res.* **2010**, *49* (13), 6196−6203.
(59) Quan, W.; Wang, X.; Song, C. Selective removal of H_2S from biogas using solid amine-based "molecular basket" sorbent. *Energy Fuels* **2017**, *31* (9), 9517−9528.
(60) Okonkwo, C. N.; Lee, J. J.; De Vylder, A.; Chiang, Y.; Thybaut, J. W.; Jones, C. W. Selective removal of hydrogen sulfide from simulated biogas streams using sterically hindered amine adsorbents. *Chem. Eng. J.* **2020**, *379*, 122349.
(61) Liu, J.; Wei, Y.; Li, P.; Zhao, Y.; Zou, R. Selective H_2S/CO_2 separation by metal−organic frameworks based on chemical-physical adsorption. *J. Phys. Chem. C* **2017**, *121* (24), 13249−13255.
(62) Belmabkhout, Y.; Pillai, R. S.; Alezi, D.; Shekhah, O.; Bhatt, P. M.; Chen, Z.; Adil, K.; Vaesen, S.; De Weireld, G.; Pang, M.; Suetin, M.; Cairns, A. J.; Solovyeva, V.; Shkurenko, A.; El Tall, O.; Maurin, G.; Eddaoudi, M. Metal−organic frameworks to satisfy gas upgrading demands: fine-tuning the soc-MOF platform for the operative removal of H_2S. *J. Mater. Chem. A* **2017**, *5* (7), 3293−3303.

https://dx.doi.org/10.1021/acsami.0c14259
ACS Appl. Mater. Interfaces XXXX, XXX, XXX−XXX